

Analysis of Cubic Niobium Thin Film Growth  
on a Sapphire Substrate Using Reflection  
High-Energy Electron Diffraction

A final report submitted in partial fulfillment of requirements  
for the degree of Bachelor of Science in Physics from the  
College of William and Mary in Virginia.

Justin Vazquez, the College of William and Mary

Advisor: Dr. Alejandra Lukaszew

Coordinator: Dr. Charles Perdrisat

Spring, 2010

## **Abstract**

The present study looked into the process of growing crystalline, thin film niobium on the surface of a sapphire substrate at ultra-high vacuum ( $<10^{-8}$  torr) and high temperature (600 °C). The overarching research goal is to eventually grow thin film niobium on the surface of more economically feasible metals, such as copper, for use in superconducting RF cavities, which are used in particle accelerators. Present technologies entail building these cavities out of pure, bulk niobium, but cost-efficient development using thin film niobium would allow for more widespread use of such accelerator devices. Growth on sapphire is well-researched and provides a good basis for understanding the growth of thin film niobium. A technique was developed for using MATLAB to perform a noise-reduced, one-dimensional line scan analysis of intensity variations along a user-defined vector in an image produced by Reflection High-Energy Electron Diffraction (RHEED). RHEED analysis gives insight into the lattice properties of the changing crystalline surface during film growth. Using this technique allowed for the determination of the orientation and atomic spacing (lattice parameters) of the niobium surface in relation to the sapphire substrate. From this analysis, it was determined that the atomic spacing on the surface of a 1 nm thin niobium film is strained by 10.11% from its relaxed bulk value at 45 nm. This likely accounts for the relaxation that takes place throughout the period of cubic niobium growth after the brief stage of initial hexagonal configuration during the first 5 to 15 Å of film growth.

## Table of Contents

|   |    |
|---|----|
| Niobium and Superconductivity.....  | 4  |
| Research Motivation: Niobium Use in Superconducting RF Cavities .....       | 4  |
| Niobium Oxidation Considerations .....                                      | 5  |
| Lattice Structures and Miller Indices .....                                 | 7  |
| Sputtering Deposition and Epitaxial Growth for Thin Films .....             | 9  |
| Thin Film Growth in the Present Study: Niobium on Sapphire and Strain ..... | 10 |
| Reflection High-Energy Electron Diffraction (RHEED) Analysis .....          | 12 |
| Analyzing RHEED Images .....  | 14 |
| Procedure and Results of the Present Study .....                            | 18 |
| Discussion and Future Directions .....                                      | 22 |
| References.....   | 23 |
| Acknowledgment .....  | 24 |

## **Niobium and Superconductivity**

Niobium (Nb, atomic number 42 on the Periodic table) is a metal with properties and reaction behavior very similar to that of Tantalum. It was, in fact, originally mistaken to be a Tantalum-based compound. Originally named "Columbium" (and still sometimes called such in American industry), this element can be used in steel alloys to aid in strength and structural integrity in the presence of frequent temperature shift, and is hence widely used in the industry.

Niobium is of great interest to the scientific community because of its being the elemental superconductor with the highest critical temperature for superconductivity (9.5 K at atmospheric pressure). This makes it possible for niobium to reach a state of superconductivity within a liquid Helium reservoir, which is relatively easily attainable in laboratory conditions. Niobium is also the 33rd most common element in the Earth's crust, giving it the additional advantage of abundance.

### **Research Motivation: Niobium Use in Superconducting RF Cavities**

As an effective superconductor, niobium can be of great use in the generation of magnetic RF fields for such devices as RF cavities for particle accelerators (i.e. the Free Electron Laser at Jefferson Lab), magnetic confinement devices (i.e. tokamaks such as the in-development ITER), and any other device that requires superconductivity to generate stable magnetic fields. The present study focuses on development of materials potentially useful in superconducting RF cavities (see Figure 1). Current technologies use bulk niobium for the entirety of the cavity makeup, but recent research has looked into the alternative method of using a *thin film* layer of niobium on the interior of the RF cavity to produce desired uniform magnetic effect.



Figure 1: A superconducting RF cavity used in the particle accelerators. (Photo courtesy the Thomas Jefferson National Accelerator Facility.)

The use of a thin film layer lining the cavity of the interior would allow the majority of the cavity to be composed of a more affordable metal, such as copper. This would make the production of such cavities much more cost efficient, and would allow for more widespread use of cavities for industrial and academic research and/or technology development and production. Such cost-efficiency is also of interest for military purposes, where there is a demand for portable, affordable accelerating devices, such as a mobile free electron laser.

### **Niobium Oxidation Considerations**

In implementing thin film Niobium as a superconductor, one faces the problem of the formation of oxide layers on metal surface. Previous studies<sup>2</sup> have shown that in standard atmospheric conditions, especially those entailing any degree of moisture in the air, niobium can

rapidly form such layers as  $\text{Nb}_2\text{O}_5$  and  $\text{NbO}$  (with growth rates as high as 0.1 nm/s under typical atmospheric conditions). These layers can be detrimental to the superconducting RF properties.

To remove these layers, a number of possible procedures can be performed. One method described in the literature<sup>2</sup> entails the use a chemical electrolysis process in which niobium is placed in a calcium bath (as shown in Figure 2); the calcium, which has a higher affinity than niobium with oxygen, will bond to the oxygen, completely removing it from the niobium surface.

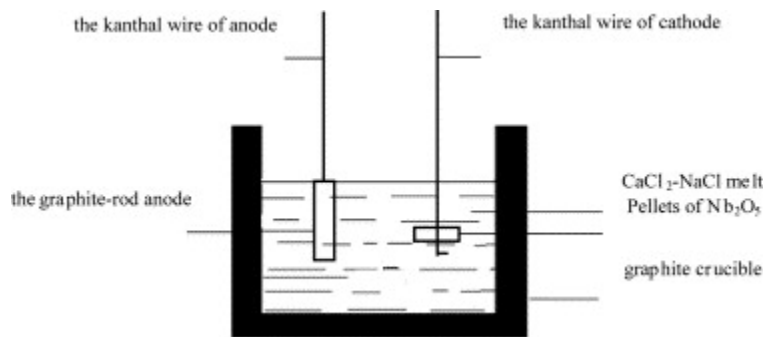


Figure 2: Schematic of a deoxidation apparatus. Removal of the oxide layer from the surface Niobium samples is often achieved by means of electrolysis in a chemical bath (Image from Ereemeev and Padamsee, 2007)

Another method of deoxidation, which is implemented in the present study, entails annealing the oxidized sample in a high-temperature, high-vacuum system. Recent studies<sup>3</sup> have shown that a significant portion of the oxide layer can be removed when a sample is placed in vacuum at 300-400 degrees Celsius ( $^{\circ}\text{C}$ ) for a number of hours. Further study<sup>4</sup> has shown that at 500  $^{\circ}\text{C}$  degrees Celsius, the top 5 nm of the surface of a niobium sample will be practically oxide-free. This is of great importance for thin film growth.

## Lattice Structures and Miller Indices

In studying crystalline thin films, understanding various lattice properties becomes essential for describing understanding the surface structure of the material being examined. In particular, for the present study, body type, Miller indices, and lattice parameters are useful properties to discuss material samples.

The type of structure, or body type, of the unit cell of a crystal lattice describes the arrangement of atoms within that lattice. This arrangement can take a number forms, including cubic, tetragonal, rhombohedral, and hexagonal. In particular, crystalline niobium will typically be arranged in a body-centered cubic (*bcc*) fashion (see in Figure 3).

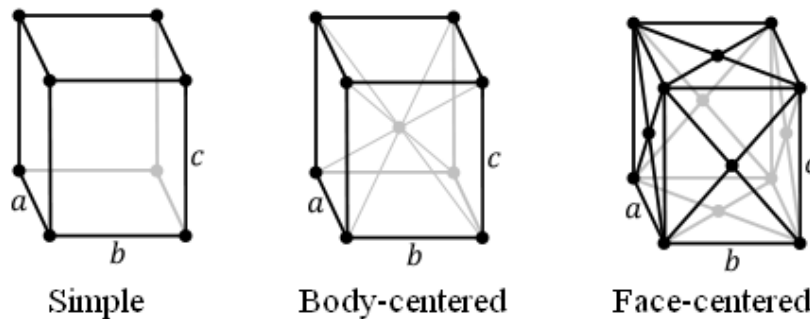


Figure 3: Types of cubic unit cells. Crystalline niobium will take on a body-centered, cubic form.

The observed crystalline surfaces of materials can be described by identifying the orientation of that surface with respect to the unit cell. This orientation can be described using Miller indices. Miller indices define a three-dimensional vector, which is normal to the cross-sectional surface observed (See figure 4). Vectors corresponding to surfaces in a *hexagonal* lattice are described by four indices, the fourth index being a redundant index which can shed light in the case of permutation symmetries.

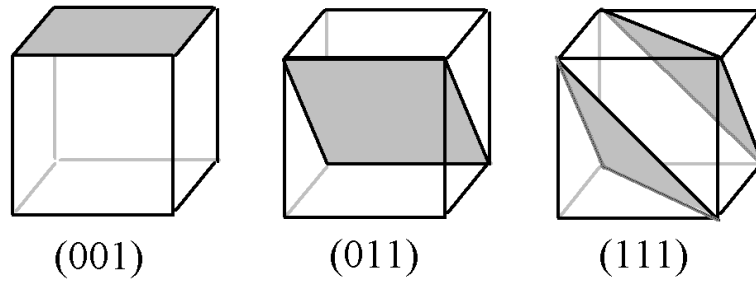


Figure 4: Examples of Miller indices and the corresponding planes they describe. The miller indices will define a vector normal to the orientation of the planar surface with respect to the unit cell.

Finally, important for crystal structure identification, especially with respect to thin film growth, are lattice parameters. These lattice parameters (as shown in Figure 5) describe the atomic spacing within the cell. For body-centered cubic niobium the lattice parameters along the 3 space directions are equal, and all angles will be  $90^\circ$ . This symmetry allows for the description of niobium using the single lattice constant  $a$ , which describes the atomic spacing on any given edge of the unity cell.

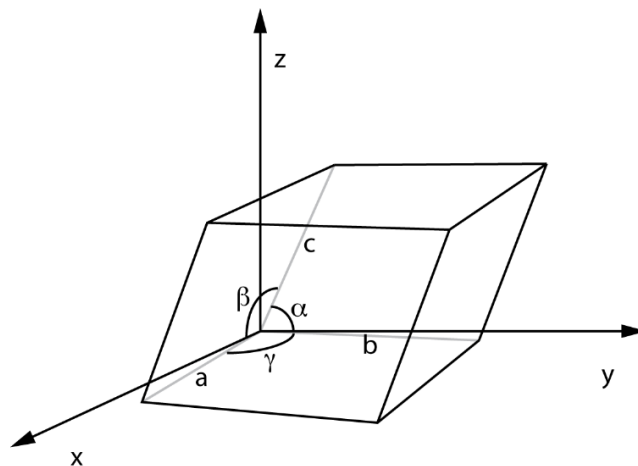


Figure 5: Schematic of lattice parameters. For cubic, body-centered niobium, all angles will be  $90^\circ$ , and all three parameters will be equal, giving way for the need to identify only one lattice constant,  $a$



## Sputtering Deposition and Epitaxial Growth for Thin Films

There are a number of methods for growing crystalline films on substrates.<sup>6</sup> The present study implemented the sputtering deposition technique. This technique (depicted in Figure 6) entails the presence of crystalline substrate on which the thin film is produced, or “grown.” The substrate is placed in an ultrahigh vacuum chamber along with a sputtering target, which is a bulk sample of the material from which the film will be composed. An ionized argon gas is then introduced to the chamber, and a negative voltage is then applied to the target. The electric potential then accelerates the ionized argon atoms towards the sputtering target. The collision of these atoms with the target knocks atoms loose from it. These released atoms then approach the substrate and settle into their most energetically favorable position. When the surface of the substrate is well-ordered and the lattice parameters of the two materials properly correspond, this settling will occur in an ordered fashion on the surface, thus forming layers of a structured, crystalline film.

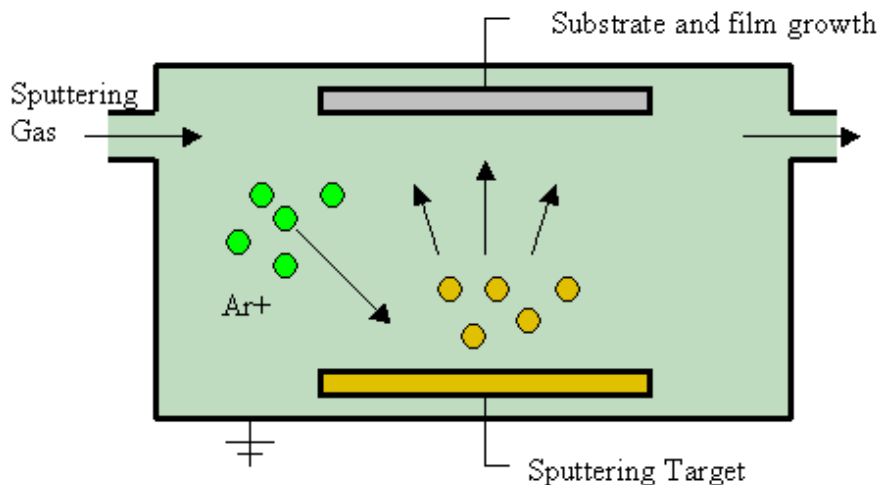


Figure 6: Schematic of a sputtering deposition apparatus used to produce thin films. Argon ions are accelerated by an applied voltage towards a sputtering target. The collision of argon with the target knocks loose atoms from the target material, which then settle on the substrate in an energetically favorable position. When this settling is well ordered, epitaxial growth occurs, and a crystalline thin film develops.

## Thin Film Growth in the Present Study: Niobium on Sapphire and Strain

In the present study, a niobium sputtering target was used to grow thin films on sapphire substrates. This particular combination was chosen because niobium is known to have lattice parameters matching well with those of sapphire, as it has been studied extensively in the past (see Wildes et. al, 2001 for a review). This allows for the growth of niobium on sapphire to be a good tool for the exploration and understanding of niobium thin film growth.

There are a number of types of epitaxial growth achievable for niobium grown on sapphire<sup>6</sup>. In this particular study, niobium was grown on A-plane ( $11\bar{2}0$ ) sapphire, forming a (110) layer (see in figure 7). Previous studies<sup>5,7</sup> have shown that, for the first 5-15 angstroms of growth, niobium will form a hexagonal structure on the sapphire surface, and then will settle into its usual body-centered cubic pattern of formation (see figure 8). The present study, however, looked only at the growth of cubic structured niobium, after the period of hexagonal growth had already ceased.

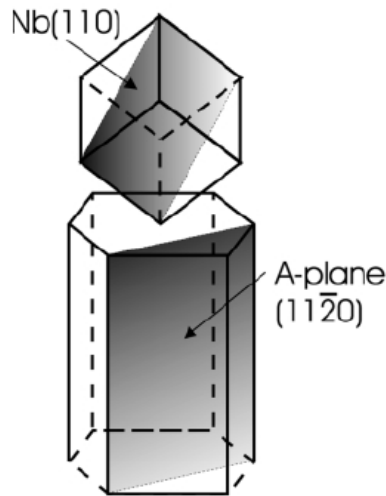


Figure 7: In the present study (110) niobium was grown on ( $11\bar{2}0$ ), a-plane sapphire. (figure adapted from Wildes et al, 2001)

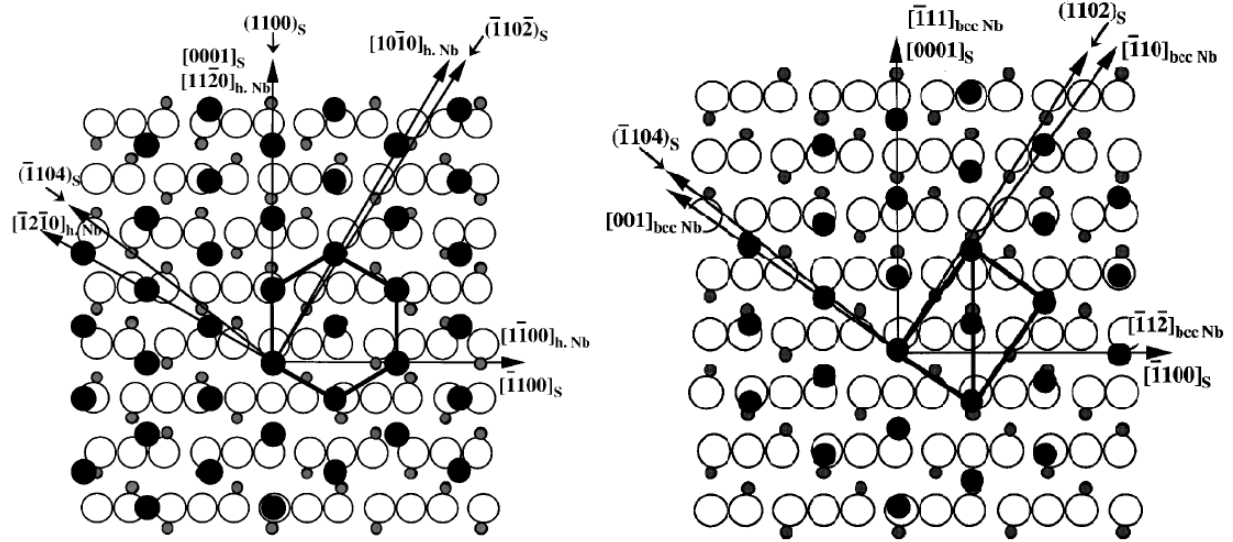


Figure 8: The first 5 to 15 Å of niobium will develop with a hexagonal structure (left) up to a critical threshold thickness, which depends on the temperature of film growth. Afterwards, it will grow with its standard cubic, body-centered form (right) (Figure adapted from Oderno et al, 1998)

While the lattice parameters of sapphire and niobium are sufficiently matched to allow for the growth of a niobium film on a sapphire substrate, they are not exactly matched. This causes the growth of the initial layers of niobium to be *strained*. This strain can be conceptualized as a stretching of the spacing between atoms from what that spacing would be for a homogeneous lattice of the given material alone, without the film-substrate interface. In addition to strain, the misalignment of lattice parameters will also be accounted for by the periodic presence of “misfit” dislocations throughout the interface surface. (See Figure 9)

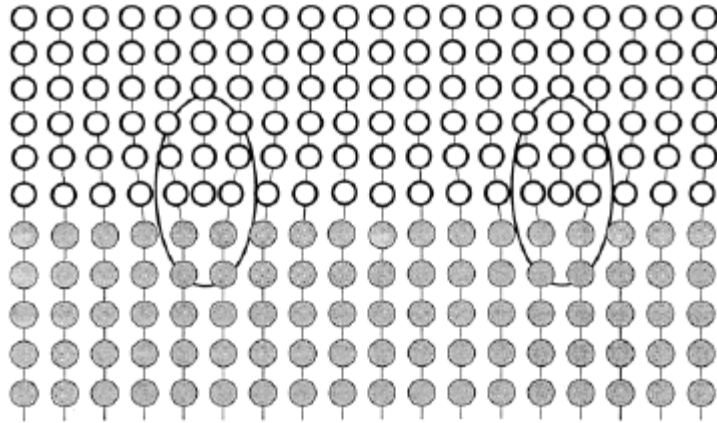


Figure 9: Niobium grown on a sapphire substrate has a lattice parameter that does not completely match that of the sapphire. Thus, the atomic spacing will initially undergo strain until it reaches a thickness where it settles into its equilibrium value. The lattice will also contain misfit dislocations (circled) to accommodate for the lattice mismatching (figure adapted from Wildes et. al, 2001)

### **Reflection High-Energy Electron Diffraction (RHEED) Analysis**

In the present study, analysis of changes to the material surface during film growth entailed use of reflection high-energy electron diffraction (RHEED) analysis. This technique entails the use of an electron beam incident on the sample surface (as depicted in Figure 10). Electrons are scattered with a diffraction pattern that corresponds to the structure and orientation of the sample surface. The electron scattering is observed on a phosphorescent screen, and information on the crystal structure can be determined. These scattering patterns correspond to the diffraction of electrons incident on the periodic surface, which can thus provide quantitative information about the surface structure.

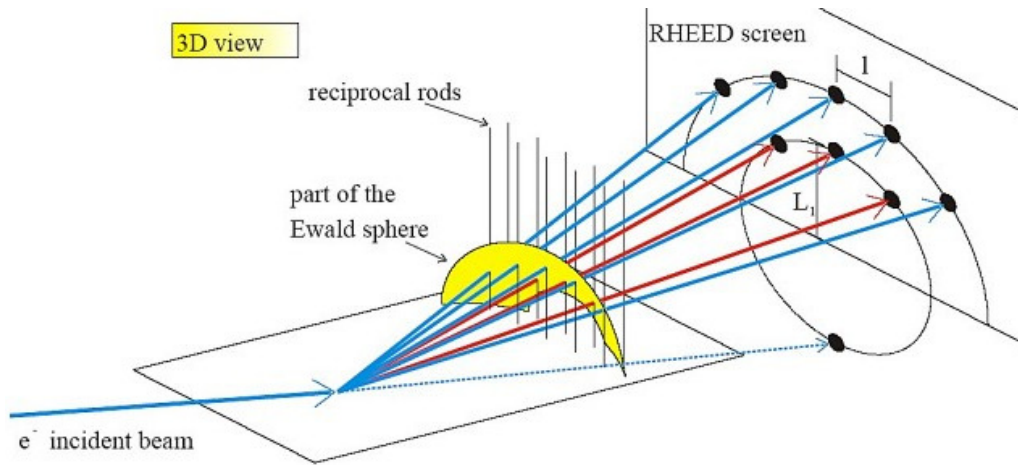


Figure 10: Schematic of the setup for RHEED analysis. An electron beam incident on the material surface will be diffracted in a manner corresponding to atomic spacing. The pattern of this diffraction will then be projected onto a phosphorescent screen.

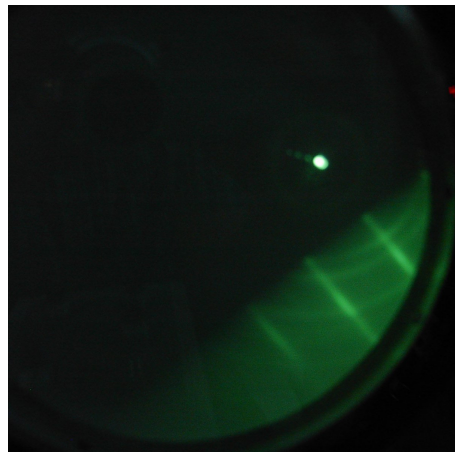


Figure 11: Example of an image observed during RHEED analysis. The diffraction pattern will contain high-intensity streaks, known as “reciprocal rods.” The spacing of these streaks will be inversely proportional to the spacing between atoms in the surface of the sample being analyzed.

## Analyzing RHEED Images

As noticeable in Figures 10 and 11 above, the basic RHEED technique (as employed in the present study) produces a series of vertical (or diagonal, depending on the orientation of the apparatus) streaks. The spacing of these streaks can be used to determine the lattice parameter corresponding to the given orientation of electron beam incidence. The general form of the relation between the two is<sup>9</sup>:

$$\frac{G}{a} = \frac{2\pi W}{\lambda L} \quad (1)$$

where  $a$  is the lattice parameter,  $W$  is the space between intensity peaks on the RHEED display,  $L$  is the horizontal distance between the electron gun and the sample being analyzed,  $\lambda$  is the DeBroglie wavelength of the electron beam, and  $G$  is a constant corresponding to the geometry of the orientation of the electron beam with respect to the crystallographic surface structure.

RHEED images thus analyzed by performing a one-dimensional line-scan to determine the intensity values along a defined user-defined line segment perpendicular to the high-intensity streaks in the image being examined. This intensity profile will contain amplitude peaks, and the spacing of these peaks can be determined and applied to determine atomic spacing. (An example of this is shown in Figure 12.)

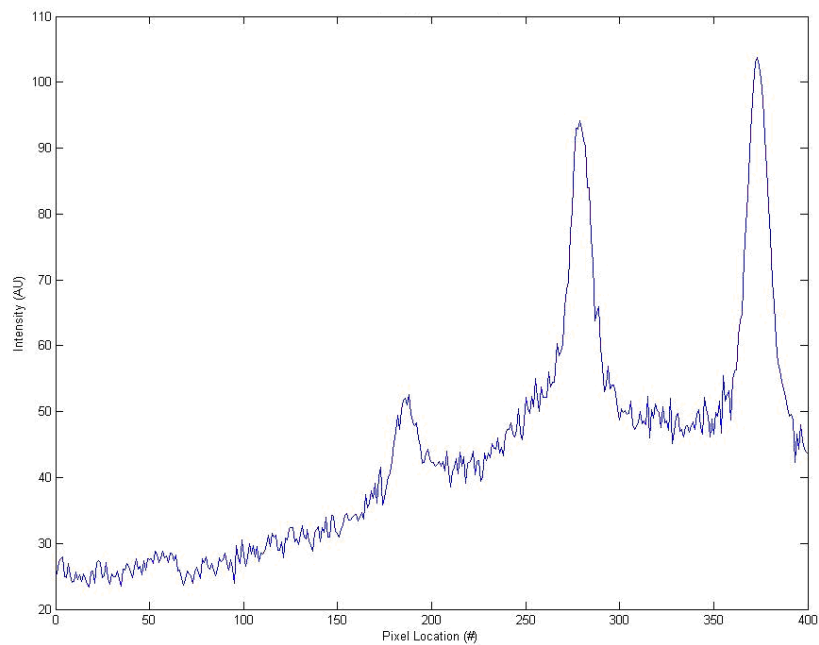
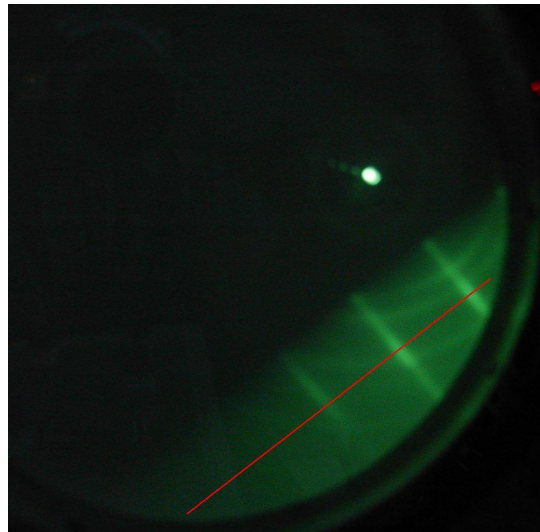


Figure 12: A line scan entails the measuring of intensity values along a user-defined line segment in the RHEED image (top). The spacing between peaks in resulting intensity profile (bottom) can then be measured to determine the spacing between the reciprocal rods.

In the present study, the line scan was performed by implementing the MATLAB Image Processing toolbox, which contains the *improfile* function. This function returns the intensity values of the pixels lying along the given line segment for the each of the RGB components. By

summing these intensity values, one can attain the values for overall intensity in the image analyzed.

In performing such a scan, however, one faces the issue of noise reduction. Because of the pixilation inherent in digitally-captured images, there is a good deal of high-frequency amplitude variation along a given vector (see Figure 13). This can make it difficult to determine the actual location of an amplitude peak along this line segment. However, if one *averages* a series of intensity scans corresponding to adjacent line segments, the randomization of the pixilation causes a cancellation of the noise, allowing for a more accurate determination of peak location.

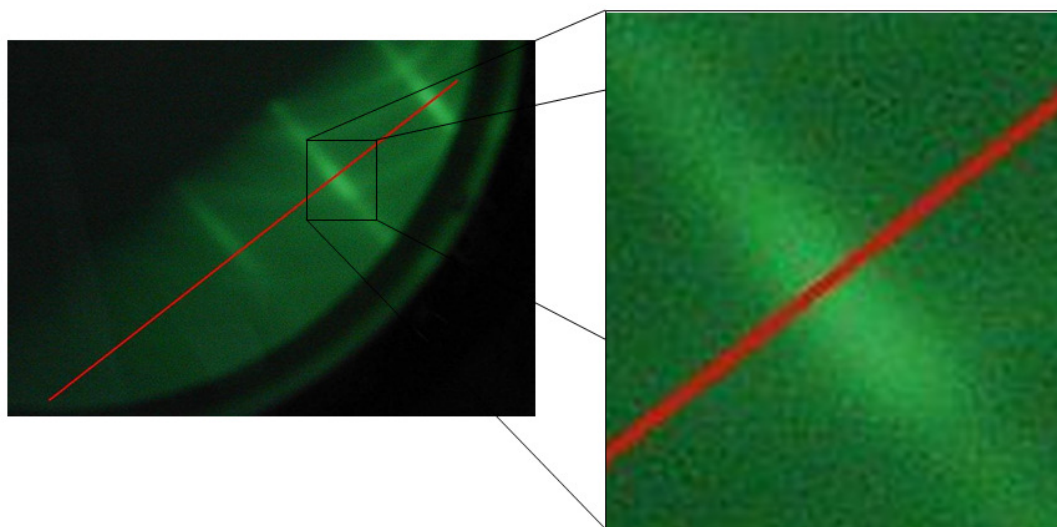


Figure 13: Pixilation in a digitally-captured RHEED image. The pixilation inherent in digital imagery creates randomized noise in the intensity values along a given vector in an image.

This method of noise cancellation was implemented in the program used in the present study. Adjacent line segments were generated in accordance with the slope perpendicular to the



original segment used for an intensity scan. This averaging thus produced a significant reduction of noise in the intensity profile. (See Figure 14)

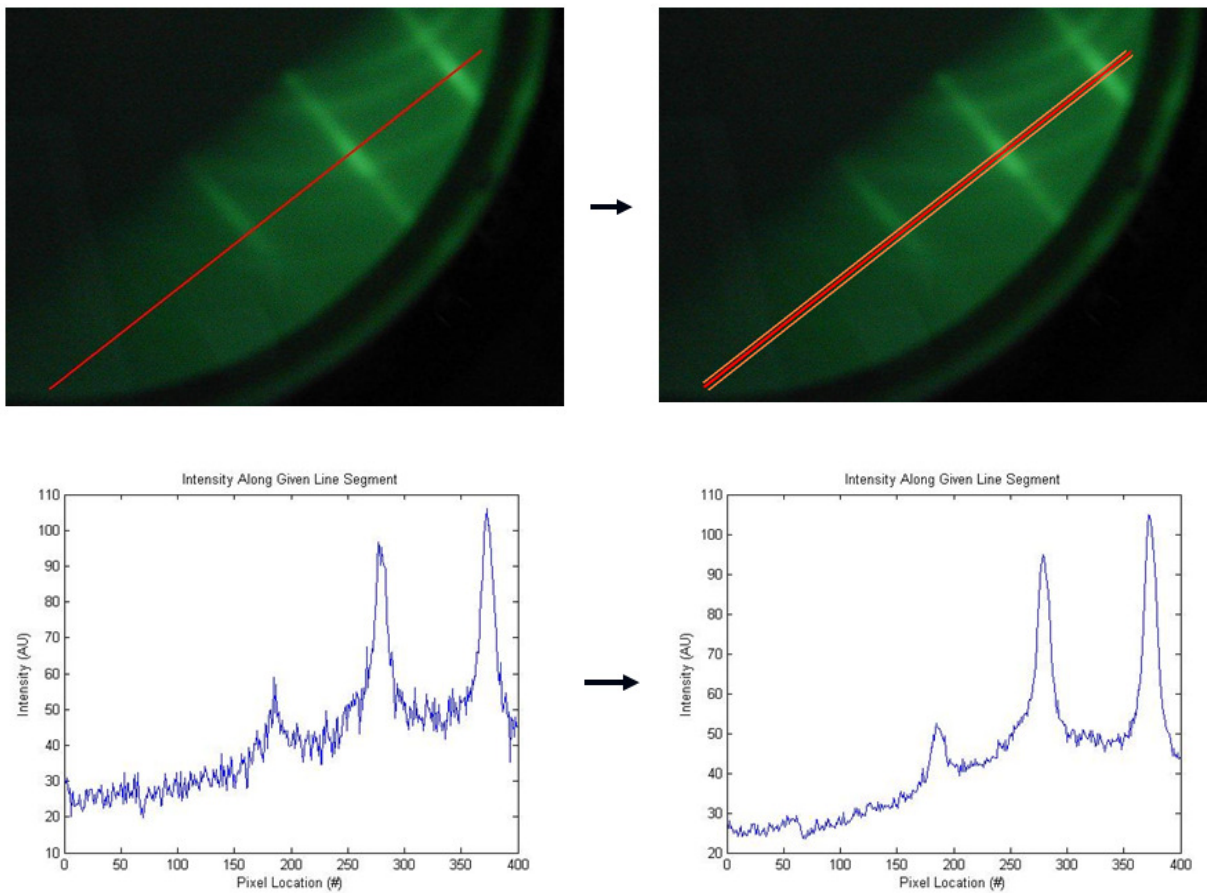


Figure 14: In the present study, noise cancellation was achieved by averaging adjacent line segments in an image (top). This averaging significant reduced the noise in the intensity profiles (bottom), allowing for effective determination of intensity peak locations. (Note: actual spacing of adjacent lines was on the order of a few pixels)

## Procedure and Results of the Present Study

In the present study, niobium growth on a sapphire substrate was performed at 600 °C, and RHEED analysis was applied for the substrate alone and for 1 nm, 2 nm, 5 nm, and 45 nm of niobium growth (at which point the film was expected to exhibit the properties of bulk niobium). The orientation of the RHEED apparatus was incident normal to the [1100] plane for sapphire, corresponding to the [112] plane for niobium. Images attained for the sapphire substrate alone appeared with the pattern as expected from previous study<sup>6</sup>, as did the images with subsequent niobium growth. (See Figures 15 and 16)

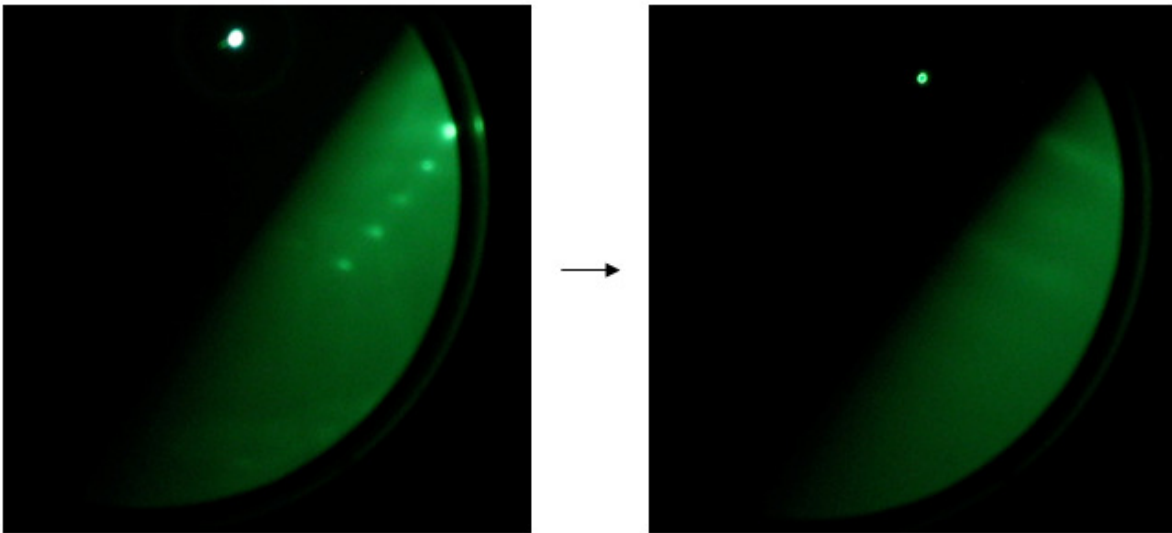


Figure 15: Changes observed in the RHEED image with the growth of niobium on sapphire. Significant changes in the diffraction pattern can be observed between the sapphire substrate (left) and the sample with 1 nm of niobium growth (right).

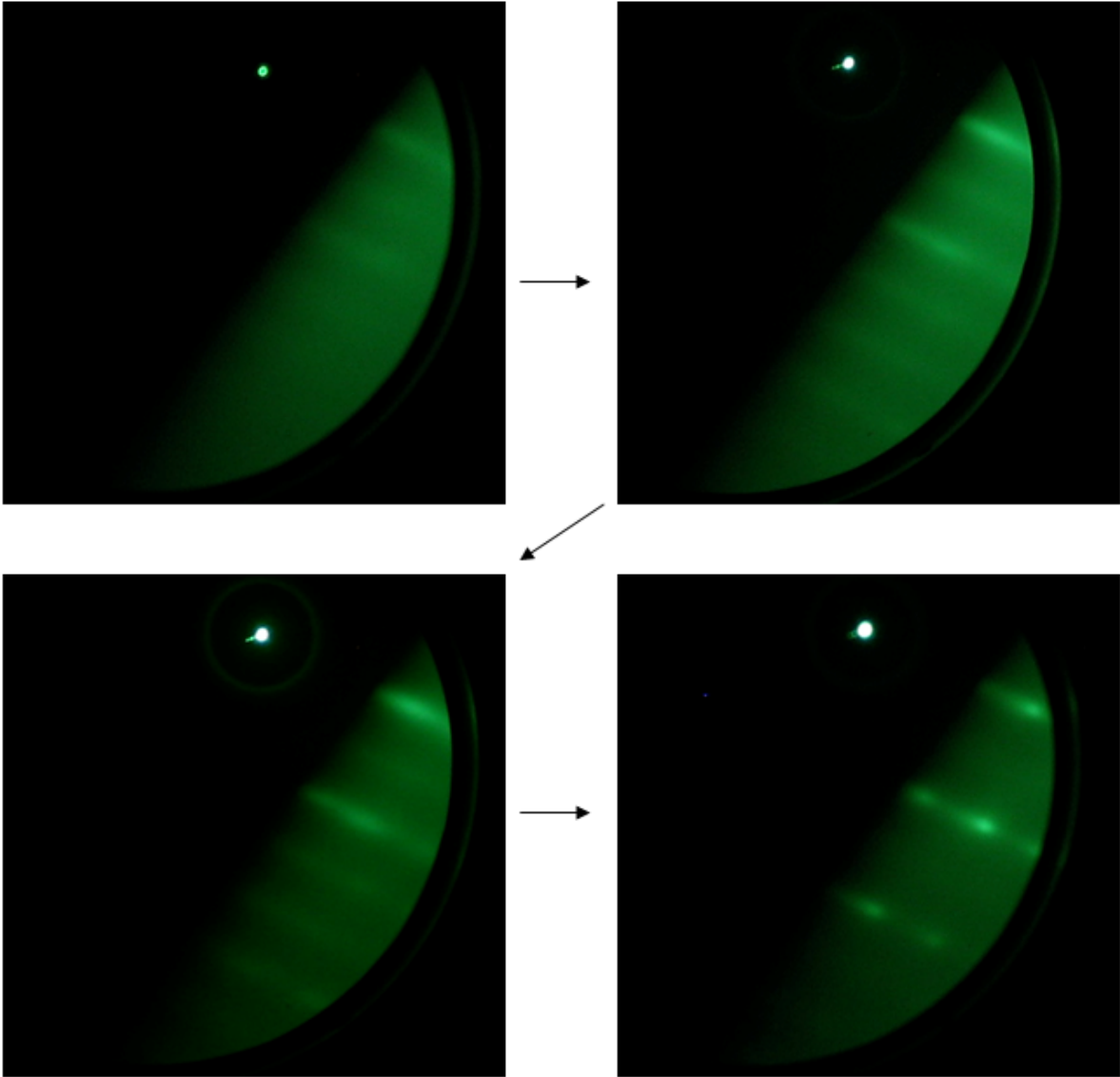


Figure 16: RHEED images observed with the presence of 1 nm (upper left), 3 nm (upper right), 5nm (lower left) and 45 nm (lower right) of niobium grown on a sapphire substrate.

One important observation is the fact that the RHEED image corresponding to 45 nm of film growth appeared to display only the brighter, more dominant intensity bands present in the other images. However, while invisible to the eye, traces of these intensity bands were apparent in the intensity scan of the image (see Figure 17).

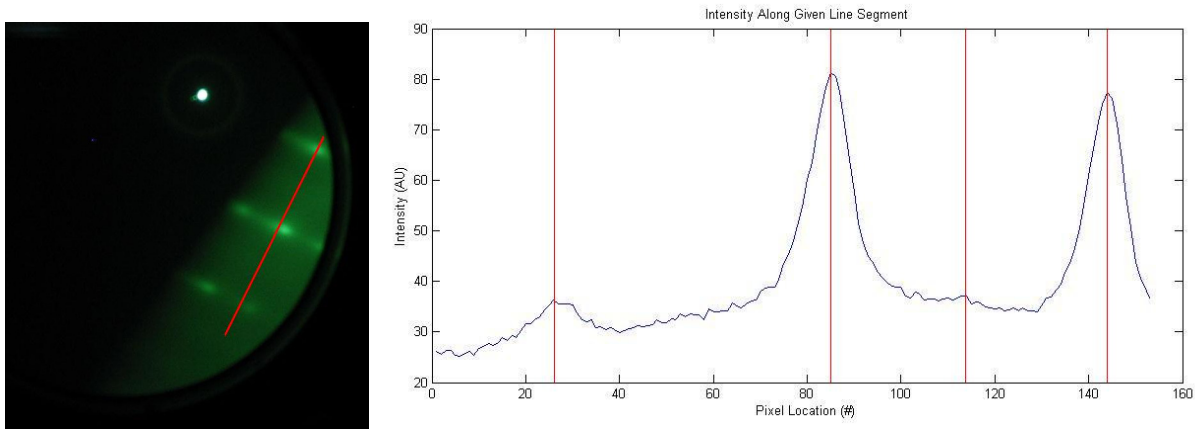


Figure 17: Intensity profile for a line scan performed on the RHEED image observed at 45 nm of niobium growth. The intensity analysis implemented shows intensity peaks (marked by vertical red lines) in the image, including some of those which are difficult to discern visually

With the RHEED images attained and intensity scans performed, the lattice constant could then be determined. For each thickness, the ratio of the peak spacing to the line-scan vector length was determined, as was the ratio of that vector length to the RHEED screen diameter. Multiplying the product of these ratios by the actual diameter of the RHEED screen (8.25 cm) gave the physical spacing of the intensity streaks. Applying Equation 1 and the geometrical factors appropriate for the particular orientation of the incident electron beam thus gave the value for the lattice constant at each given film thickness.

The expected lattice constant for bulk niobium, with correction for thermal expansion, was  $3.457\text{\AA}$ . The experimental measure of this constant, corresponding to the measure with 45 nm of niobium growth, was  $3.630\text{\AA}$ . The error between the two was 5.00%, and given the systematic errors in measuring the geometry of the apparatus, it could be assumed that 45 nm of growth corresponded to niobium having reached its bulk state with nearly complete relaxation of the strain. For thick enough niobium films, the lattice parameter is supposed to be completely relaxed to the bulk value. Thus, the 45 nm thick film could be used for calibration of the RHEED

apparatus, its lattice parameter corresponding to the lattice constant for bulk niobium with correction for thermal expansion,  $3.457\text{\AA}$ .

The lattice constants measured at the various film thicknesses of niobium are shown in Figure 18. After growing from 1 nm of niobium to 45 nm, the measured lattice constants relaxed from a strained value of  $3.997\text{\AA}$  to  $3.630\text{\AA}$ . (In calibrated terms, this relaxation was from a strained value  $3.807\text{\AA}$  to  $3.457\text{\AA}$ ). This suggests that, with 1 nm of growth on the sapphire substrate, the spacing of niobium atoms in the film is strained by 10.11% from the relaxed, bulk value.

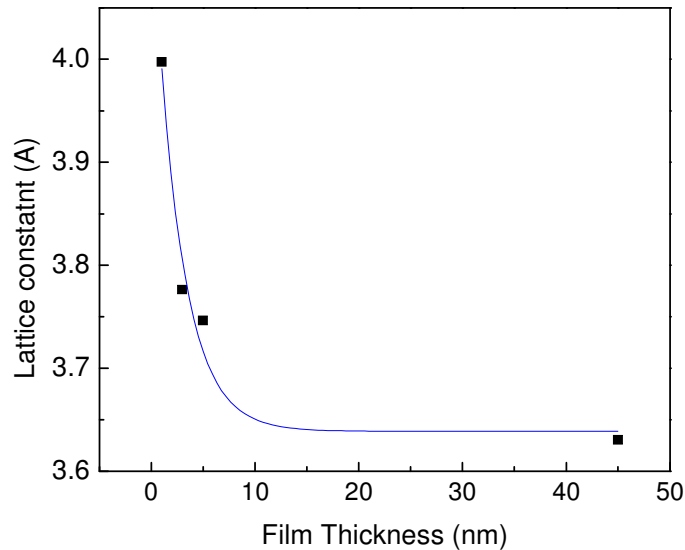


Figure 18: The lattice parameters of various thicknesses of thin film niobium grown on a sapphire substrate. As expected these values leveled off exponentially to an equilibrium value. This bulk lattice constant was within about 5% of the expected value at  $600\text{ }^{\circ}\text{C}$ . (The exponential fit displayed serves merely to provide a guide to the eye.

Further investigation would provide a more accurate fit for the data.)

## Discussion and Future Directions

The present study investigated the strain relaxation of niobium thin films produced by sputtering deposition at 600 °C in ultra high vacuum conditions. A method of producing a noise-reduced analysis of images acquired while using the RHEED technique was developed and applied to images captured for various film thicknesses during the growth process. While strong lattice strain was observed for thinner niobium films, lattice parameters for thicker films were found to be closer to the expected bulk value. A niobium film with a thickness of 1 nm was found to have a lattice parameter strained by 10.11% from that of a 45 nm thick film, which was treated as the bulk value.

Previous studies<sup>5</sup> have suggested that 10 Å (1 nm) of film growth is just above the threshold for the transition from hexagonal to cubic niobium growth at 600 °C. Hence, the percentage of strain observed on the film surface at 1 nm of niobium growth versus 45 nm of growth could correspond to the overall degree of relaxation that takes place during the period of cubic-structured niobium growth in niobium thin film production on a sapphire substrate. Further research into thinner niobium films, however, will be necessary to fully assert this.

Future studies may entail the development of better analyzing techniques, particularly better noise reduction. For example, a Fourier analysis-based reduction of certain frequencies of amplitude variation could improve the capability of peak determination, removing the need for line averaging. Also useful will be more automated program activity for image output, peak spacing determination, and user interface.

Future studies into the period of cubic niobium growth could also entail more detailed acquirement of RHEED images and determination of lattice parameters. More detailed observation of the growth period between 5 nm and 45 nm of niobium growth, and perhaps

beyond 45 nm, could allow determination of thickness at which the spacing niobium atoms relaxes to its bulk value. Detailed value measurements of atomic spacing could also then be related to superconducting characteristics of niobium thin films at various film thicknesses.

The study of growth on a sapphire substrate is the initial step in understanding and working with the growth and analysis techniques discussed. Successful implementation and understanding of these techniques will allow for further understanding of the crystallographic characteristics of niobium at thin film thickness. Relating these characteristics to its superconductive properties could be useful in the development and implementation of thin film niobium superconductors.

Eventually, research will look further into niobium growth on other material substrates. Of particular interest for potential use in superconducting RF cavities is growth on other conductive metals, such as copper. Previous studies have already begun to look into niobium thin film growth on copper (eg. Mašek and Matolin, 2001), but further research and understanding will be valuable for the successful implementation and integration of nano-scale thin film and particle acceleration technologies.

## References

1. J. Halbritter, *Applied Physics A Solids and Surfaces*, 43 (1987)1.
2. R. O. Suzuki, M. Aizawa and K. Ono, *Journal of Alloys and Compounds*, 288 (1999) 173.
3. G. Eremeev and H. Padamsee, *Proceedings of SRF2007*, Peking Univ., Beijing, China (2007) 356.
4. R. Kirby, F. K King King, F K and H Padamsee, *SLAC-TN 05* (2005)
5. V. Oderno, C. Dufour, K. Dumesnil, A. Mougín, Ph. Mangin and G. Marchal, *Philosophical Magazine Letters* 78 (1998) 419.
6. A. R. Wildes, J. Mayer and K. Theis-Bröhl, *Thin Solid Films* 401 (2001) 7.

7. R. C. C. Ward, E. J. Grier and A. K. Petford-Long, *Journal of Materials Science: Materials in Electronics*, 14 (2003) 533.
8. K. Mašek and V Matolin, *Vacuum*. 61 (2001) 217.
9. J. E. Mahan, K. M. Geib, G. Y. Robinson and R. G. Long, *J. Vac. Sci. Technol. A* 8 (1990) 3692

### **Acknowledgement**

This research is performed collaboratively with the Department of Energy Office of High Energy Physics via the Thomas Jefferson National Accelerator Facility under United States Department of Energy Contract No. DE-AC05-06OR23177